

YAJING ZHANG<sup>1,3</sup>  
YU ZHANG<sup>1</sup>  
FU DING<sup>1,3</sup>  
KANGJUN WANG<sup>1,3</sup>  
XIAOLEI WANG<sup>2</sup>  
BAOJIN REN<sup>1</sup>  
JING WU<sup>1</sup>

<sup>1</sup>College of Chemical Engineering,  
Shenyang University of Chemical  
Technology, Shenyang, China

<sup>2</sup>School of Science, Shenyang  
University of Technology,  
Shenyang, China

<sup>3</sup>Liaoning Co-innovation Center of  
Fine Chemical Industry, Shenyang,  
China

SCIENTIFIC PAPER

UDC 66.094.25:546.264–31:544.47

<https://doi.org/10.2298/CICEQ150711005Z>

## SYNTHESIS OF DME BY CO<sub>2</sub> HYDROGENATION OVER La<sub>2</sub>O<sub>3</sub>-MODIFIED CuO-ZnO-ZrO<sub>2</sub>/HZSM-5 CATALYSTS

### Article Highlights

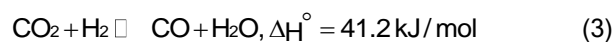
- La-modified CuO-ZnO-ZrO<sub>2</sub>/HZSM-5 catalysts were prepared by an oxalate co-precipitation method
- La-modified CuO-ZnO-ZrO<sub>2</sub>/HZSM-5 catalysts show higher catalytic performances
- The catalytic performances of the catalysts are strongly dependent on the La content

### Abstract

A series of La<sub>2</sub>O<sub>3</sub>-modified CuO-ZnO-ZrO<sub>2</sub>/HZSM-5 catalysts were prepared by an oxalate co-precipitation method. The catalysts were fully characterized by X-ray diffraction (XRD), N<sub>2</sub> adsorption-desorption, hydrogen temperature programmed reduction (H<sub>2</sub>-TPR), ammonia temperature programmed desorption (NH<sub>3</sub>-TPD), and X-ray photoelectron spectroscopy (XPS) techniques. The effect of the La<sub>2</sub>O<sub>3</sub> content on the structure and performance of the catalysts was thoroughly investigated. The catalysts were evaluated for the direct synthesis of dimethyl ether (DME) from CO<sub>2</sub> hydrogenation. The results displayed that La<sub>2</sub>O<sub>3</sub> addition enhanced catalytic performance, and the maximal CO<sub>2</sub> conversion (34.3%) and DME selectivity (57.3%) were obtained over the catalyst with 1% La<sub>2</sub>O<sub>3</sub>, which due to the smaller size of Cu species and a larger ratio of Cu<sup>+</sup>/Cu.

Keywords: CO<sub>2</sub> hydrogenation; dimethyl ether; La<sub>2</sub>O<sub>3</sub> promoter.

Carbon dioxide emission has caused irreversible climate changes due to its greenhouse effect [1]. CO<sub>2</sub> capture and storage is one of efficient method for reducing the CO<sub>2</sub> emissions. However, this technology requires high cost [2]. Chemical recycling of CO<sub>2</sub> is another main option, which is presented as an economically attractive and sustainable method. CO<sub>2</sub> can be converted into methanol, dimethyl ether (DME), methane and syngas (CO+H<sub>2</sub>) [3], carboxylic acids, etc. Among them, synthesis of DME has been paid special attention since DME can be applied as a clean fuel, coolant, propellant, and is an important chemical intermediate [4]. The chemical reactions occurring in direct conversion of CO<sub>2</sub> to DME can be described by the following equations [5]:



For the methanol synthesis (reaction (1)), CuO-ZnO-ZrO<sub>2</sub> catalytic system is considered as more favorable than the traditional CuO-ZnO-Al<sub>2</sub>O<sub>3</sub>, because the interaction of Cu metal particles with ZnO and ZrO<sub>2</sub> lead to the stabilization of a “mix” of Cu and Cu<sup>δ+</sup> (not Cu<sup>2+</sup>, Cu<sup>1+</sup> and Cu) [6]. For the methanol dehydration process (reaction (3)), solid-acid catalysts (HZSM-5, γ-Al<sub>2</sub>O<sub>3</sub> and sulfated zirconia) are employed [7]. HZSM-5 is widely applied for methanol dehydration because: 1) it has very high catalytic activity at the optimum reaction temperature; 2) it is more resistant toward poisoning of acid sites by the water due to more hydrophobic character; 3) predominance of Brønsted-type acidity, which can promote the DME yield [8]. However, H-ZSM-5 presents the disadvantages of narrow pore size and strong acid sites, which

Correspondence: F Ding, K. Wang, College of Chemical Engineering, Shenyang University of Chemical Technology, Shenyang 110142, PR China.

E-mail: F. Ding, [dingfu@syuct.edu.cn](mailto:dingfu@syuct.edu.cn);  
K. Wang, [angle\\_79@163.com](mailto:angle_79@163.com)

Paper received: 11 July, 2015

Paper revised: 8 January, 2016

Paper accepted: 19 February, 2016

will limit reactant molecules diffusion and lead to formation of secondary products, respectively. Witton *et al.* developed sulfated zirconia catalyst with 20% sulfur-loaded on ZrO<sub>2</sub> as methanol dehydration catalyst, the yield of methanol and DME over CuO-ZnO-ZrO<sub>2</sub>/20S-ZrO<sub>2</sub> both higher than those over CuO-ZnO-ZrO<sub>2</sub>/H-ZSM-5, but the stability of the former catalyst is a little poor [9].

Up to now, the conversion of CO<sub>2</sub> and the selectivity of DME are still not high. To enhance the catalytic activity, efforts have been addressed by adding promoters for methanol synthesis catalyst, besides developing new preparation methods [10–14]. Our previous results showed that V and Mn oxides modified CuO-ZnO-ZrO<sub>2</sub>/HZSM-5 exhibited higher catalytic performance [15–16]. La<sub>2</sub>O<sub>3</sub>, as a rare earth metal oxide, is considered as owing some basic character [17], and it can promote many metal oxide catalytic reactions. Guo *et al.* [18] investigated catalysis performance of La doping Cu/ZrO<sub>2</sub> for CO<sub>2</sub> hydrogenation to methanol, and they found the amount of basic site increases with La loading and the presence of La enhance the selectivity of methanol. Gao *et al.* reported appropriate amount of La can decrease the crystallite size of CuO and enhance the dispersion of Cu [19]. Sun's group has investigated the effect of La on the performance of Cu/Zn/Al catalysts via hydroxalcalite-like precursors for CO<sub>2</sub> hydrogenation to methanol, and the results showed La addition not only led to higher BET specific surface area and Cu dispersion, but also increased the total number of basic sites and proportion of strongly basic sites [20]. Furthermore, Sun's group also reported that addition of Zr to La-Cu-Zn-O with perovskite structure catalyst, for synthesis of methanol from CO<sub>2</sub> hydrogenation, will lead to smaller particles, lower reduction temperature, higher Cu dispersion, larger amount of hydrogen desorption at low temperature as well as higher concentration of basic sites are obtained [21]. However, the introduction of La<sub>2</sub>O<sub>3</sub> into the CuO-ZnO-ZrO<sub>2</sub>/HZSM-5 catalyst for CO<sub>2</sub> to DME has not been reported.

Herein, La<sub>2</sub>O<sub>3</sub>-modified CuO-ZnO-ZrO<sub>2</sub>/HZSM-5 catalysts with a different La<sub>2</sub>O<sub>3</sub> content were prepared, aiming at investigating the effect of La<sub>2</sub>O<sub>3</sub> modification on the structure and performance the catalysts.

## EXPERIMENTAL

### Catalyst preparation

The La<sub>2</sub>O<sub>3</sub> modified CuO-ZnO-ZrO<sub>2</sub>/HZSM-5 (CuO:ZnO:ZrO<sub>2</sub> mass ratio: 5:4:0.2) catalysts, abbrevi-

ated as CZZLxH where *x* stands for theoretical La<sub>2</sub>O<sub>3</sub>/CZZ wt.%, were prepared by an oxalate co-precipitation method (CZZLx/HZSM-5 mass ratio: 2:1), HZSM-5 (SiO<sub>2</sub>/Al<sub>2</sub>O<sub>3</sub> mole ratio: 50) was purchased from Catalyst Plant of Nankai University (China). The preparation method is same as described in other work [15]. In brief, first, metal nitrates were dissolved into a certain amount of ethanol (denoted as solution A); H<sub>2</sub>C<sub>2</sub>O<sub>4</sub>·2H<sub>2</sub>O (200 mol.% of metal nitrate) was also dissolved into ethanol (solution B). Then, solutions A and B were slowly dropped into a beaker containing a HZSM-5 suspension in ethanol suspension kept under stirring at 333 K. The suspension was sealed and aged for 2 h and then the ethanol was evaporated at 353 K to get a precipitate. Finally, the precipitate was dried at 393 K for 12 h and calcined in air at 673 K for 4 h.

### Catalyst testing

Catalytic performance was evaluated in a continuous-flow fixed-bed reactor made of stainless steel with inside diameter of 0.01 m. First, the catalyst was reduced with 10% H<sub>2</sub>/N<sub>2</sub> at 573 K for 3 h under atmospheric pressure. Then it was cooled to 653 K and reactant gas flow was introduced, raising the pressure to 3.0 MPa, the reaction temperature was 543 K. The exit line was heated to prevent condensation. The products were analyzed on line with a gas chromatograph (SP2100A) equipped with both a TCD (for CO and CO<sub>2</sub>, GDX-101 connected with Porapak T column) and a FID (for CH<sub>4</sub>, CH<sub>3</sub>OH and CH<sub>3</sub>OCH<sub>3</sub>, Porapak Q column). Conversion and selectivity values were calculated by internal standard method [22].  $X_{\text{CO}_2}$ ,  $S_{\text{pi}}$  and  $Y_{\text{DME}}$  represent the conversion of CO<sub>2</sub>, the selectivity of the product (DME, MeOH and CO) and the yield of DME, respectively. Each experimental data was corresponds to an average of three independent measurements, with error of ±2%.

$$X_{\text{CO}_2} = \frac{\text{CO}_{2,\text{in}}/N_{2,\text{in}} - \text{CO}_{2,\text{out}}/N_{2,\text{out}}}{\text{CO}_{2,\text{in}}/N_{2,\text{in}}} \quad (4)$$

$$S_{\text{pi}} = \frac{P_i}{1 - \text{CO}_{2,\text{out}}} \quad (5)$$

where  $P_i$  stands for the concentration of a specific *i* product (DME, MeOH or CO):

$$Y_{\text{DME}} = S_{\text{DME}} X_{\text{CO}_2} \quad (6)$$

### Catalyst characterization

XRD measurements were performed on a Rigaku D/max 2500pc X-ray diffractometer with Cu-K $\alpha$

radiation ( $\lambda = 1.54156 \text{ \AA}$ ) at a scan rate of  $4^\circ \text{ min}^{-1}$  at 50 kV and 250 mA. For the reduced catalysts were first reduced with 10% H<sub>2</sub>/N<sub>2</sub> at 573 K for 3 h, and cooled to room temperature under the N<sub>2</sub> flow, and then keep it into a bottle full of N<sub>2</sub> and send it to XRD chamber immediately. The crystallite size was calculated using the Scherrer equation. BET surface areas were measured by N<sub>2</sub> adsorption at 77 K using a Quantachrome Autosorb 1-C. Before measurements, samples were degassed under vacuum at 573 K for 4 h. H<sub>2</sub>-TPR was carried out in 10% H<sub>2</sub>/Ar flowing at 50 mL min<sup>-1</sup>, using a ramp rate of 10 K min<sup>-1</sup> to 773 K. NH<sub>3</sub>-TPD was conducted on a Chemisorb from 373 to 873 K. XPS measurements were performed on an ESCALAB-250. The catalysts were first reduced with 10% H<sub>2</sub>/N<sub>2</sub> at 573 K for 3 h, and cooled to room temperature under the N<sub>2</sub> flow, then put into the chamber of X-ray photoelectron spectrometer immediately for measurement. The exact composition of the surface of the catalyst was determined by XPS. Acidity on the catalyst was measured on a NICOLET 500 FT-IR through pyridine adsorption. The sample was prepared to the load slice, which was subject to purification under vacuum pressure 0.0133 Pa at 673 K, after cooling down to the room temperature, pyridine was adsorbed for 0.5 h. Desorption was carried out by programming temperature to 423 K. The infrared spectrum was generated within the scope of 1400–1700 cm<sup>-1</sup> at room temperature.

## RESULTS AND DISCUSSION

### Catalytic performance of catalysts

The catalytic performances of CZZL<sub>x</sub>H catalysts with varying La<sub>2</sub>O<sub>3</sub> content are summarized in Table 1. The major product was DME, and the side products were methanol, CO and trace hydrocarbons. The amount of hydrocarbons was less than 1% and therefore they were neglected. The CO<sub>2</sub> conversions and DME selectivities over the La<sub>2</sub>O<sub>3</sub>-modified catalysts are higher than those over unmodified one (CZZL<sub>0</sub>H), indicating that La<sub>2</sub>O<sub>3</sub>-modification can efficiently enhance the catalytic performances. The CZZL<sub>1</sub>H exhibited the maximum CO<sub>2</sub> conversion and DME sel-

ectivity of 34.3 and 57.3%, respectively. CO<sub>2</sub> conversion over CZZL<sub>1</sub>H increases 18.6%, compared with CZZL<sub>0</sub>H. The influence of the catalyst composition on the performance does not seem distinct, which is due to the thermodynamic regime of reaction test because of combination of high temperature and long contact time. If the temperature is decreased to 533 K, the differences of conversion and DME selectivity between CZZL<sub>1</sub>H and CZZL<sub>0</sub>H become much larger (Table 2). It is also noted that the selectivity of CO is high (about 30%), which may due to the higher reaction temperature of 543 K. CO was produced by reverse water-gas reaction, the reaction has endothermic character, as shown in reaction (2). Meanwhile, compared to methanol synthesis, the RWGS reaction has a higher apparent activation energy [23], indicating that the increase in CO production is faster than that of methanol with higher reaction temperature. The selectivity of CO over CZZL<sub>1</sub>H exhibited the minimal value, indicating that a certain amount of La<sub>2</sub>O<sub>3</sub> can inhibit the RWGS reaction. However, as Gao *et al.* pointed out, further work needs to be carried out to investigate how La<sub>2</sub>O<sub>3</sub> changes the RWGS reaction [19].

In order to further increase the DME yield, the catalytic performance of the CZZL<sub>1</sub>H catalyst was also investigated at lower gas hourly space velocity. As shown in Table 2, when the GHSV was as low as 1800 h<sup>-1</sup>, the CO<sub>2</sub> conversion and DME selectivity increase to 36.4 and 58.2%, respectively. The increase of the conversion can be attributed to the longer contact time of CO<sub>2</sub> and H<sub>2</sub> over the catalyst at lower GHSV. Similarly, methanol dehydration can proceed to a higher degree with increasing contact time, leading to higher DME selectivity. In addition, a contrast experiment was carried out at a reaction pressure of 5 MPa while keeping other conditions constant. DME selectivity increased by approximately 7.3% and CO selectivity decreased by 24.6% compared with those obtained at 3 MPa. This result suggests that an increase of reaction pressure can improve the catalytic performance.

### The structure of catalyst

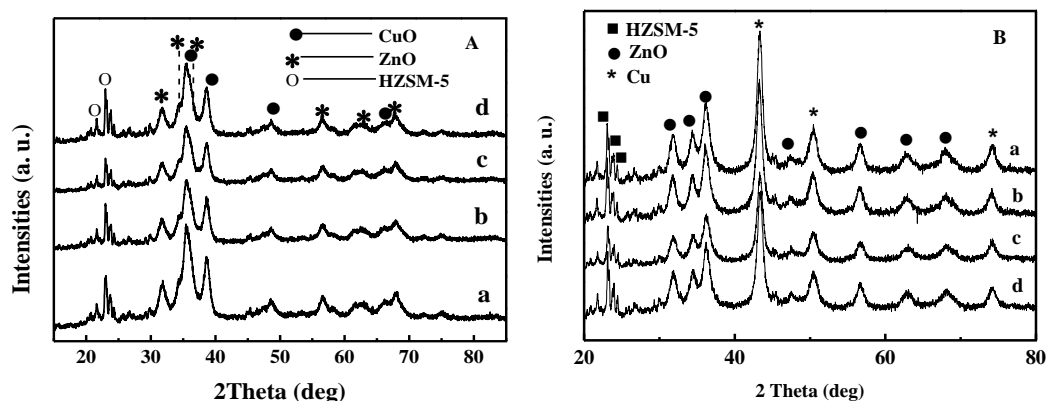
Figure 1A shows the XRD patterns of CZZL<sub>x</sub>H catalysts. The peaks appearing at 35.5, 38.7, 48.7,

Table 1. Catalytic performances of the catalysts; reaction conditions:  $T = 543 \text{ K}$ ;  $p = 3.0 \text{ MPa}$ ;  $\text{CO}_2:\text{H}_2 = 1:3$ ;  $\text{GHSV} = 4200 \text{ h}^{-1}$

Catalyst	Conversion of CO <sub>2</sub> , %	Selectivity, %			DME Yield, %	DME Productivity, g g cat <sup>-1</sup> h <sup>-1</sup>
		DME	CH <sub>3</sub> OH	CO		
CZZL <sub>0</sub> H	28.9	55.1	12.9	32.0	15.9	0.171
CZZL <sub>0.5</sub> H	30.4	55.2	12.4	31.7	16.8	0.181
CZZL <sub>1</sub> H	34.3	57.3	13.3	29.4	19.6	0.212
CZZL <sub>2</sub> H	31.1	53.6	12.7	33.7	16.7	0.180

Table 2. Catalytic performances of the catalysts at different reaction conditions; reaction conditions: CO<sub>2</sub>:H<sub>2</sub> = 1:3

Catalyst	T K	Conversion of CO <sub>2</sub> %	p MPa	GHSV h <sup>-1</sup>	Selectivity, %			DME Yield %	DME Productivity g g cat <sup>-1</sup> h <sup>-1</sup>
					DME	CH <sub>3</sub> OH	CO		
CZZL <sub>1</sub> H	543	34.3	3	4200	57.3	13.3	29.4	19.6	0.212
CZZL <sub>1</sub> H	543	36.4	3	1800	58.2	14.2	27.6	21.1	0.098
CZZL <sub>1</sub> H	543	38.5	5	1800	62.5	16.7	20.8	24.0	0.111
CZZL <sub>0</sub> H	533	24.2	3	4200	57.1	13.7	29.2	13.8	0.148
CZZL <sub>1</sub> H	533	30.4	3	4200	61.8	14.2	24.0	18.8	0.203

Figure 1. A) XRD patterns of La<sub>2</sub>O<sub>3</sub>-modified CuO-ZnO-ZrO<sub>2</sub>/HZSM-5 and B) reduced catalysts: a) CZZL<sub>0</sub>H; b) CZZL<sub>0.5</sub>H; c) CZZL<sub>1</sub>H; d) CZZL<sub>2</sub>H.

and 66.2° can be ascribed to CuO phase (tenorite, JCPDS 48-1548), the peaks at 31.7, 34.3, 36.6, 56.5, 62.8 and 67.8° can be indexed to ZnO phase (JCPDS 65-3411), and the peaks appearing in the 2θ range of 21–25° belong to HZSM-5 (JCPDS 44-0003). No peaks belonging to ZrO<sub>2</sub> or La<sub>2</sub>O<sub>3</sub> are observed, indicating that ZrO<sub>2</sub> and La<sub>2</sub>O<sub>3</sub> are amorphous or well dispersed in catalyst body. The intensities of the peaks assigned to CuO and ZnO weakened and the widths of the peaks broadened gradually with increasing La<sub>2</sub>O<sub>3</sub> content from 0 to 1%, then they became sharper and narrower again when La<sub>2</sub>O<sub>3</sub> content was 2%. This result indicates that the addition of a proper amount of La<sub>2</sub>O<sub>3</sub> can enhance the dispersion of CuO and ZnO [24]. This changing trend can be well reflected in the changing trends of Cu and CuO grain size, as shown in Table 3.

Table 3. Physicochemical properties of the catalysts; diffraction peak at 2θ 38.7° for CuO and 43.3° for Cu

Catalyst	S <sub>BET</sub> / m <sup>2</sup> g <sup>-1</sup>	D <sub>XRD</sub> / nm	
		CuO	Cu
CZZL <sub>0</sub> H	135.4	11.3	13.5
CZZL <sub>0.5</sub> H	136.7	9.6	11.9
CZZL <sub>1</sub> H	138.2	8.4	10.5
CZZL <sub>2</sub> H	135.8	9.3	11.4

The XRD patterns of the reduced catalysts are shown in Figure 1B. The diffraction peaks at 2θ values of 43.3, 50.4 and 74.1° can be indexed to the crystal planes of (111), (200) and (220) of metallic copper phase, respectively (JCPDS 04-0836). No diffraction peaks belonging to the CuO phase could be detected, suggesting all CuO species had been reduced to copper. The intensities of the peaks assigned to Cu and ZnO changed in a similar trend as those of CuO and ZnO (Figure 1A).

The specific surface areas and the calculated crystallite sizes of the catalysts using Scherrer's equation are listed in Table 3. The S<sub>BET</sub> increased from 135.4 of CZZL<sub>0</sub>H to 138.2 m<sup>2</sup> g<sup>-1</sup> of CZZL<sub>1</sub>H, and then decreased to 135.8 m<sup>2</sup> g<sup>-1</sup> for CZZL<sub>2</sub>H. The changing trend of the D<sub>Cu</sub> is opposite to the trend of the S<sub>BET</sub>, a minimum of 10.5 nm is obtained over CZZL<sub>1</sub>H. Although the S<sub>BET</sub> change is not as significant as D<sub>Cu</sub>, the trend is in accordance with XRD results. Combining the results in both Tables 1 and 3, it can be observed that CZZL<sub>1</sub>H shows the smallest Cu crystallite size and the best catalytic performance, which indicates the activity is closely related to the crystallite size of Cu. Guo *et al.* also reported the catalytic performance of Cu-TiO<sub>2</sub>-ZrO<sub>2</sub> related to the crystallite size of CuO [25].

### The reducibility of catalyst

H<sub>2</sub>-TPR results are depicted in Figure 2. It is obvious that La<sub>2</sub>O<sub>3</sub> modification displays a significant effect on the interaction between the metal and the carriers. Each catalyst exhibits a broad peak with peak maximum in 423–563 K, corresponding to the reduction of CuO to Cu [26]. For the catalysts with increasing La<sub>2</sub>O<sub>3</sub> content from 0 to 0.5 or 1%, the peaks maxima shift to higher temperature from 529 to 554 or 556 K while no shape changes are observed, which indicates the interaction between ZnO and CuO or La<sub>2</sub>O<sub>3</sub> and CuO becomes stronger [19,23,27]. This result seems conflicting with XRD result. According to XRD result, the dispersion of CuO becomes better and the crystalline size becomes gradually smaller with La<sub>2</sub>O<sub>3</sub> addition amount from 0 to 1%, suggesting that the reducibility of CuO should become easier. This fact implies La<sub>2</sub>O<sub>3</sub> modification still plays another role. For CZZL<sub>2</sub>H catalyst, it is evident that the H<sub>2</sub>-TPR change tendency becomes more different and the peak maximum shifts towards the lower temperature, indicating the reducibility of CuO becomes easier [28,29]. It is concluded that La<sub>2</sub>O<sub>3</sub> modification has at least two roles. On one hand, La modification promotes the dispersion of CuO, leading to easier reduction of CuO; on the other hand, La<sub>2</sub>O<sub>3</sub> modification enhances the interaction between CuO and other metal oxides resulting in a more difficult reduction process. The two effects compete with each other and the reduction temperature is dependent on which effect is predominant. Xiong *et al.* also found that the La<sub>2</sub>O<sub>3</sub> can increase the dispersion of Co/AC catalysts, whereas the reduction temperature shifted to a higher position due to stronger interaction [30].

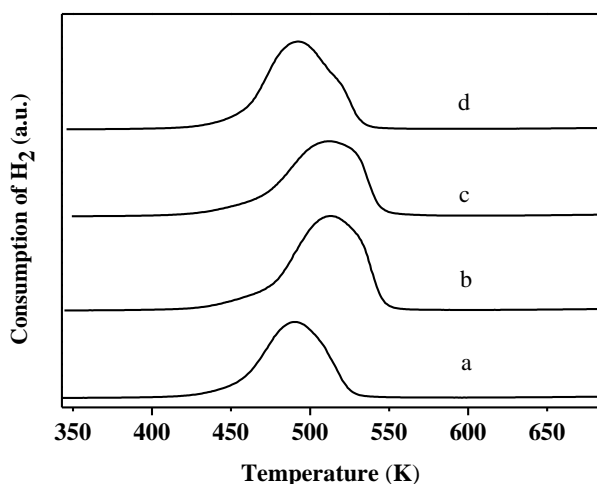


Figure 2. H<sub>2</sub>-TPR profiles of catalysts: a) CZZL<sub>0</sub>H; b) CZZL<sub>0.5</sub>H; c) CZZL<sub>1</sub>H; d) CZZL<sub>2</sub>H.

### Surface acidity of catalyst

Figure 3 shows the NH<sub>3</sub>-TPD results obtained for pure HZSM-5 and CZZL<sub>x</sub>H catalysts. The total acidic amount, the strength and the fraction of various acid sites are summarized (supporting info, available from the authors upon request). On pure HZSM-5 profile, two NH<sub>3</sub> desorption peaks are observed, indicating the existence of at least two different acid strengths. In general, the peak located in 393–523 K and 573–773 K can be attributed to weak and strong acid strengths, respectively [31]. But for all catalysts, three NH<sub>3</sub> desorption peaks, in the temperature regions of 373–473 K, 473–573 K and 573–673 K are observed, denoted as  $\alpha$ ,  $\beta$  and  $\gamma$  peak, which can be assigned to weak, medium and strong acid strengths of HZSM-5, respectively [32]. This result is similar with that of the reported V-modified catalyst [15]. According to the study, the reason why the catalysts showed another more NH<sub>3</sub> desorption peak than pure HZSM-5 is mainly ascribed to the fact that strong acid strength on pure HZSM-5 are blocked and modified by metal oxides and oxalic acid, respectively. Compared with La<sub>2</sub>O<sub>3</sub>-free catalyst, peaks  $\alpha$  and  $\beta$  on the other curves shift a little to higher temperature with the increasing La<sub>2</sub>O<sub>3</sub> content, implying that the weak and medium acid strengths become stronger; on the contrary, the peak  $\gamma$  shifts a little towards lower temperature, indicating strong acid strength becomes weaker. It is also worth noting that the total acid amount decreases with the increasing amount of La<sub>2</sub>O<sub>3</sub> from 0.5 to 1%, which can be explained by the basic character of La<sub>2</sub>O<sub>3</sub>. Sugi *et al.* also observed this effect and suggested that La<sub>2</sub>O<sub>3</sub>-modification resulted in reducing the support acidity [33]. However, continuous addition of La<sub>2</sub>O<sub>3</sub> to 2% increases the total

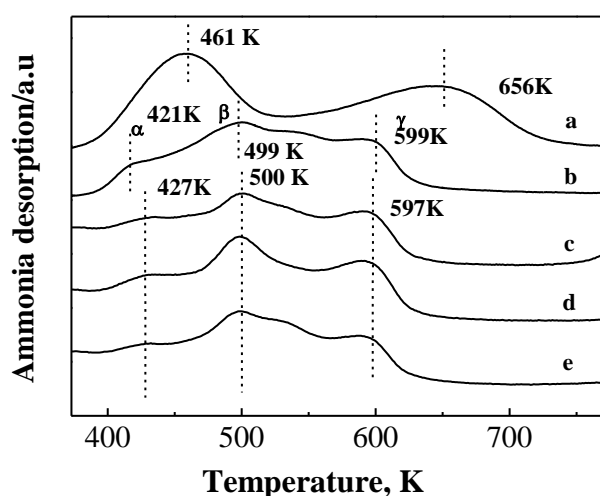


Figure 3. NH<sub>3</sub>-TPD profiles of pure HZSM-5 and the catalysts: a) HZSM-5; b) CZZL<sub>0</sub>H; c) CZZL<sub>0.5</sub>H; d) CZZL<sub>1</sub>H; e) CZZL<sub>2</sub>H.

acid amount again. Previously published studies proposed that there are two reasons for the acidity amount increase [34]. One is that the La<sup>3+</sup> has some Lewis acidic property originated from an empty f orbital; the other reason is that Si-OH and Al-OH in the zeolite framework are polarized by La<sup>3+</sup>, which result in a stronger acidity. Therefore, the acidity of the CZZLxH catalysts is dependent on the La<sub>2</sub>O<sub>3</sub> content.

Moreover, La<sub>2</sub>O<sub>3</sub> modification can also affect the concentration and distribution of the three acid strengths of HZSM-5 in the catalysts. With the increasing amount of La<sub>2</sub>O<sub>3</sub>, the concentration and fraction of medium acid strength increase and those of strong acid strength become smaller as compared to those on CZZL<sub>0</sub>H, but the difference is too small (supporting info). It is generally considered that the strong acidic strength on HZSM-5 zeolite promotes the generation of secondary products like hydrocarbons, resulting in low selectivity to DME [6]. However, here the change of the acidity could not be a factor accounting for the higher DME selectivity because the methanol selectivity of the various catalysts was almost the same, as shown in Table 1. This result suggests that the acidity of the catalysts is strong enough to efficiently convert the produced methanol to DME. In addition, the acidity of Brønsted acid sites and Lewis acid sites for CZZL<sub>0</sub>H and CZZL<sub>1</sub>H catalysts were determined (supporting info, available from the authors upon request). The results show the acidity of both type acid sites of CZZL<sub>1</sub>H decreased compared CZZL<sub>0</sub>H, thus it can be inferred that there is no direct relationship between the selectivity of DME and the change of acid type of the two catalysts. So, the improvement of DME selectivity is due to the decrease in CO selectivity resulted from the Cu-based catalyst but not from the acid component of the bifunctional catalysts. In addition, according to the literature, it could be speculated that the introduction of La<sub>2</sub>O<sub>3</sub> into catalyst will increase the surface basicity of catalyst, which in turn promotes the adsorption of CO<sub>2</sub> and sequence enhances the yield for methanol, finally DME selectivity is increased after methanol dehydration [18].

### Results of XPS investigations

The reduced CZZLxH catalysts characterized by XPS, the binding energy of Cu2p<sub>3/2</sub>, Zn2p<sub>3/2</sub>, as well as the surface compositions of the catalysts are summarized (supporting info, available from the author upon request). For all the reduced catalysts, binding energies (BE) of Cu2p<sub>3/2</sub> are located at about 932.3 eV, which are the characteristic peaks of reduced Cu<sup>+</sup>/Cu species [35]. The binding energy shifted to

higher positions with increasing amounts of La<sub>2</sub>O<sub>3</sub>, which indicated stronger interaction between CuO and other metal oxides carriers [36]. For the purpose of distinguishing Cu<sup>+</sup> from Cu species, their kinetic energies in the XAES Cu LMM line positions were measured (Figure 4). The Cu LMM spectra show a broad and asymmetrical peak, implying the coexistence of Cu<sup>+</sup> and Cu in the surface of the catalysts. Two symmetrical peaks centered at near 916.6 and 918.7 eV can be obtained by deconvolution, which are corresponding to Cu<sup>+</sup> and Cu species, respectively [37]. Additionally, Cu<sup>+</sup>/Cu can be calculated based on the results. Volcanic shape change trends of the Cu<sup>+</sup>/Cu *versus* La addition content are observed, the CZZL<sub>1</sub>H exhibited the maximum of 0.144, which may consequently lead to higher activity due to the stabilization of Cu<sup>+</sup> favoring the hydrogenation of CO<sub>2</sub> [38]. The binding energies (BE) of Zn2p<sub>3/2</sub> for all catalysts are located at about 1021.8 eV, which are close to the characteristic peaks of ZnO species [39]. Compared to the nominal surface compositions of the catalysts, it can be seen that the actual surface composition Cu/Zn decreased significantly, implying enrichment of Zn. Similarly, La<sub>2</sub>O<sub>3</sub> content is much higher on the surface. It is worth noting that is La<sub>2</sub>O<sub>3</sub> is not detectable in CZZL<sub>0.5</sub>H, possibly because the content is too small to give enough signal.

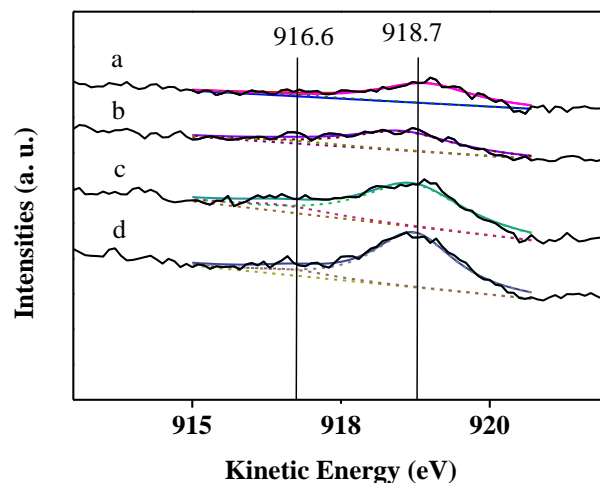


Figure 4. Cu LMM XAES spectra of the reduced catalysts: a) CZZL<sub>0</sub>H; b) CZZL<sub>0.5</sub>H; c) CZZL<sub>1</sub>H; d) CZZL<sub>2</sub>H.

### CONCLUSIONS

La<sub>2</sub>O<sub>3</sub> modification has great impact on the catalytic performance of CuO-ZnO-ZrO<sub>2</sub>/HZSM-5 catalysts for promoting direct CO<sub>2</sub>-to-DME. La<sub>2</sub>O<sub>3</sub>-modification can efficiently enhance the catalytic performance of CuO-ZnO-ZrO<sub>2</sub>/HZSM-5 catalysts. The sample containing a nominal amount of 1% La<sub>2</sub>O<sub>3</sub>

gave the maximum CO<sub>2</sub> conversion and DME selectivity of 34.3 and 57.3%, respectively, benefiting from smaller Cu particles and a larger Cu<sup>+</sup>/Cu ratio. When the La<sub>2</sub>O<sub>3</sub> content is low (from 0.5 to 1%), it can strengthen the interaction between CuO and other metal oxides and inhibit the reduction of CuO species; meanwhile, the total acid amount decreases slightly but the medium strong acid concentration and strength increase a little. However, excess of La<sub>2</sub>O<sub>3</sub> content, *e.g.*, 2%, will lead to an opposite effect. In summary, suitable La<sub>2</sub>O<sub>3</sub> addition can improve the catalytic performance of CuO-ZnO-ZrO<sub>2</sub>/HZSM-5 for one step CO<sub>2</sub> to DME transformation.

### Acknowledgement

The authors thank National Nature Science Foundation of China (51301114, 21201123, 21203125 and 61403263), SRF for ROCS, SEM (No. [2010]1174), Natural Science Foundation of Liaoning Province (2015020649), Liaoning Educational Department Foundation (L2013161), LNET (LJQ2013044) for financial support.

### REFERENCES

- [1] P. Cox, C. Jones, *Science* **321** (2008) 1642-1644
- [2] S.C.G. Santos, S.W.M. Machado, A.M. Garrido Pedrosa, M.J.B. Souza, *J. Porous Mater.* **22** (2015) 1145-1151
- [3] A. García-Trenco, A. Vidal-Moya, A. Martínez, *Catal. Today* **179** (2012) 43-51
- [4] T.A. Semelsberger, K.C. Ott, R.L. Borup, H.L. Greene, *Appl. Catal., A: Gen.* **309** (2006) 210-223
- [5] G. Bonura, M. Cordaro, C. Cannilla, A. Mezzapica, L. Spadaro, F. Arena, F. Fusteri, *Catal. Today* **228** (2014) 51-57
- [6] T. Takeguchi, K. Yanagisawa, T. Inui, M. Inoue, *Appl. Catal., A: Gen.* **192** (2000) 201-209
- [7] T. Witoo, S. Bumrungsalee, M. Chareonpanich, J. Limtrakul, *Energy Conv. Manage.* **103** (2015) 886-894
- [8] A. García-Trenco, A. Martínez, *Appl. Catal., A: Gen.* **411-412** (2012) 170-179
- [9] T. Witoo, T. Permsirivanich, N. Kanjanasontorn, C. Akkaraphataworn, A. Seubsai, K. Faungnawakij, C. Warakulwit, M. Chareonpanich, J. Limtrakul, *Catal. Sci. Technol.* **5** (2015) 2347-2357
- [10] L. Shi, K. Tao, R.Q. Yang, F.Z. Meng, C. Xing, N. Tsubaki, *Appl. Catal., A: Gen.* **401** (2011) 46-55
- [11] P. Gao, F. Li, F. K. Xiao, N. Zhao, W. Wei, L.S. Zhong, Y.H. Sun, *Catal. Today* **194** (2012) 9-15
- [12] F. Zha, J. Ding, Y. Chang, J.F. Ding, J.Y. Wang, J. Ma, *Ind. Eng. Chem. Res.* **51** (2012) 345-352
- [13] X.M. Guo, D.S. Mao, G.Z. Lu, S. Wang, G.S. Wu, *J. Mol. Catal., A: Chem.* **345** (2011) 60-68
- [14] J. Xiao, D.S. Mao, X.M. Guo, J. Yu, *Energy Technol.* **3** (2015) 32-39
- [15] Y.J. Zhang, D.B. Li, Y. Zhang, Y. Cao, S.J. Zhang, K.J. Wang, F. Ding, J. Wu, *Catal. Commun.* **55** (2014) 49-52
- [16] Y.J. Zhang, D.B. Li, D. Jiang, Y. Zhu, Y. Wu, S. Zhang, K. Wang, *J. Mol. Catal. (China)* **28** (2014) 344-350
- [17] K. Wakui, K. Satoh, G. Sawada, K. Shiozawa, K. Matano, K. Suzuki, Y. Yoshimura, T. Hayakawa, K. Murata, F. Mizukami, *Catal. Lett.* **81** (2002) 83-88
- [18] X.M. Guo, D.S. Mao, G.Z. Lu, S. Wang, G.S. Wu, *J. Mol. Catal., A: Chem.* **345** (2011) 60-68
- [19] W.G. Gao, H. Wang, Y.H. Wang, W. Guo, M.Y. Jia, *J. Rare Earths* **31** (2013) 370-375
- [20] P. Gao, F. Li, N. Zhao, F.K. Xiao, W. Wei, L.S. Zhong, Y.H. Sun, *Appl. Catal., A: Gen.* **468** (2013) 442-452
- [21] H.J. Zhan, F. Li, P. Gao, N. Zhao, F.K. Xiao, W. Wei, L.S. Zhong, Y.H. Sun, *J. Power Sources* **251** (2014) 113-124
- [22] G. Bonura, M. Cordaro, L. Spadaro, C. Cannilla, F. Arena, F. Frusteri, *Appl. Catal., B: Environ.* **140-141** (2013) 16-24
- [23] L. Li, D.S. Mao, J. Yu, X.M. Guo, *J. Power Sources* **279** (2015) 394-404
- [24] S.G. Li, H.J. Guo, C.R. Luo, H.R. Zhang, L. Xiong, X.D. Chen, L.L. Ma, *Catal. Lett.* **143** (2013) 345-355
- [25] X.M. Guo, D.S. Mao, S. Wang, G.S. Wu, G.Z. Lu, *Catal. Commun.* **10** (2009) 1661-1664
- [26] R. Nie, H. Lei, S. Pan, L. Wang, J. Fei, Z. Hou, *Fuel* **96** (2012) 419-425
- [27] P. Gao, F. Li, H.J. Zhan, N. Zhao, F.K. Xiao, W. Wei, L.S. Zhong, *J. Catal.* **298** (2013) 51-60
- [28] R.W. Liu, Z.Z. Qin, H.B. Ji, T.M. Su, *Ind. Eng. Chem. Res.* **5** (2013) 16648-16655
- [29] Y.W. Zhang, Y.M. Zhou, H. Liu, Y. Wang, Y. Xu, P.C. Wu, *Appl. Catal., A: Gen.* **323** (2007) 202-210
- [30] G.P. Jiao, Y.J. Ding, H.J. Zhu, X.M. Li, W.D. Dong, J.W. Li, Y. Lv, *J. Catal. (China)* **30** (2009) 92-94
- [31] C.V. Hidalgo, H. Itoh, T. Hattori, M. Niwa, Y. Murakami, *J. Catal.* **45** (1984) 362-370
- [32] G. Bonura, M. Cordaro, L. Spadaro, C. Cannilla, F. Arena, F. Frusteri, *Appl. Catal., B: Environ.* **140-141** (2013) 16-24
- [33] Y.Y. Shu, D. Ma, X.H. Bao, Y. Xu, *Catal. Lett.* **66** (2000) 161-167
- [34] X.N. Wang, Z. Zhao, C.M. Xu, A.J. Duan, L. Zhang, G.Y. Jiang, *J. Rare Earths* **25** (2007) 321-328
- [35] P.H. Matter, D.J. Braden, U.S. Ozkan, *J. Catal.* **223** (2004) 340-351
- [36] J.M. Camposmartin, A. Guerrerorruiz, J.L.G. Fierro, *J. Catal.* **156** (1995) 208-218
- [37] K.P. Sun, W.W. Lu, F.Y. Qiu, X.L. Xu, *Appl. Catal., A: Gen.* **252** (2003) 243-249
- [38] D.S. Mao, W.M. Yang, J.C. Xia, B. Zhang, Q.Y. Song, Q.L. Chen, *J. Catal.* **230** (2005) 140-149
- [39] D.G. Cantrell, L.J. Gillie, A.F. Lee, K. Wilson, *Appl. Catal., A: Gen.* **287** (2005) 183-190.

YAJING ZHANG<sup>1,3</sup>  
YU ZHANG<sup>1</sup>  
FU DING<sup>1,3</sup>  
KANGJUN WANG<sup>1,3</sup>  
XIAOLEI WANG<sup>2</sup>  
BAOJIN REN<sup>1</sup>  
JING WU<sup>1</sup>

<sup>1</sup>College of Chemical Engineering,  
Shenyang University of Chemical  
Technology, Shenyang, China

<sup>2</sup>School of Science, Shenyang Univer-  
sity of Technology, Shenyang, China

<sup>3</sup>Liaoning Co-innovation Center of Fine  
Chemical Industry, Shenyang, China

NAUČNI RAD

## SINTEZA DIMETIL ETRA HIDROGENIZACIJOM CO<sub>2</sub> POMOĆU LA<sub>2</sub>O<sub>3</sub>-MODIFIKOVANIH CuO-ZnO-ZrO<sub>2</sub>/HZSM-5 KATALIZATORA

*Oksalatnom ko-precipitacionom metodom je pripremljena serija katalizatora CuO-ZnO-ZrO<sub>2</sub>/HZSM-5 modifikovanih pomoću La<sub>2</sub>O<sub>3</sub>. Katalizatori su okarakterisani X-difrakcionom metodom (XRD), N<sub>2</sub> adsorpcijom-desorpcijom, termoprogramiranom redukcijom (H<sub>2</sub>-TPR), termoprogramiranom desorpcijom (NH<sub>3</sub>-TPD) i fotoelektronskom spektroskopijom X-zraka (XPS). Istražen je i uticaj sadržaja La<sub>2</sub>O<sub>3</sub> na strukturu i performanse katalizatora. Katalizatori su testirani u procesu CO<sub>2</sub> hidrogenizacije i direktne sinteze dimetil etra (DME). Rezultati pokazuju da dodatak La<sub>2</sub>O<sub>3</sub> poboljšava performanse katalizatora, kao i da su maksimalna konverzija CO<sub>2</sub> (34,3%) i DME selektivnost (57,3%) dobijeni upotrebom katalizatora sa 1% La<sub>2</sub>O<sub>3</sub>, zbog manjih Cu čestica i većeg odnosa Cu<sup>+</sup>/Cu<sup>0</sup>.*

*Ključne reči: hidrogenizacija CO<sub>2</sub>, dimetil etar La<sub>2</sub>O<sub>3</sub> promoter.*